

Evidence that mechanisms of fin development evolved in the midline of early vertebrates

Renata Freitas¹, GuangJun Zhang¹ & Martin J. Cohn^{1,2}

The origin of paired appendages was a major evolutionary innovation for vertebrates, marking the first step towards fin- (and later limb-) driven locomotion. The earliest vertebrate fossils lack paired fins but have well-developed median fins^{1,2}, suggesting that the mechanisms of fin development were assembled first in the midline. Here we show that shark median fin development involves the same genetic programs that operate in paired appendages. Using molecular markers for different cell types, we show that median fins arise predominantly from somitic (paraxial) mesoderm, whereas paired appendages develop from lateral plate mesoderm. Expression of *Hoxd* and *Tbx18* genes, which specify paired limb positions^{3,4}, also delineates the positions of median fins. Proximodistal development of median fins occurs beneath an apical ectodermal ridge, the structure that controls outgrowth of paired appendages⁵⁻⁷. Each median fin bud then acquires an anteroposteriorly-nested pattern of *Hoxd* expression similar to that which establishes skeletal polarity in limbs^{8,9}. Thus, despite their different embryonic origins, paired and median fins utilize a common suite of developmental mechanisms. We extended our analysis to lampreys, which diverged from the lineage leading to gnathostomes before the origin of paired appendages^{2,10}, and show that their median fins also develop from somites and express orthologous *Hox* and *Tbx* genes. Together these results suggest that the molecular mechanisms for fin development originated in somitic mesoderm of early vertebrates, and that the origin of paired appendages was associated with re-deployment of these mechanisms to lateral plate mesoderm.

Outgrowth of paired fins and limbs is maintained by the apical ectodermal ridge (AER) at the distal margin of the buds^{5,6}, and members of the Fgf family synergistically mediate its signalling activity^{7,11}. In catsharks, median fins develop from a continuous finfold extending along the dorsal and ventral midlines (Supplementary Fig. 1). Outgrowth of the median finfold occurs beneath an AER-like structure that produces Fgf8 and Dlx proteins (Supplementary Fig. 2). The AER then becomes an apical ectodermal fold (AEF), as in the paired fins of teleosts⁶. The similar embryology of median and paired fins raised the possibility that a common set of mechanisms regulates their development, but their anatomical positions suggested distinctive embryonic origins. Transplantation experiments in amphibians have led to the idea that median finfolds are neural crest derived, and the zebrafish caudal fin was shown to originate, at least in part, from trunk neural crest^{12,13}. Recent fate-mapping studies, however, demonstrated that somitic mesoderm contributes to amphibian median finfold development¹⁴. We therefore set out to determine the embryonic origin of catshark median fins.

Studies in several model systems have shown that *Foxc2* and *Zic1* are expressed in the sclerotome, and that they remain in these cells as they migrate dorsally around the neural tube to form neural arches and spinous processes^{15,16}. Neither of these genes is expressed by

migratory trunk neural crest or differentiated myotome^{15,16}, making them suitable for distinguishing sclerotomal cells during median fin development. We cloned and examined the expression of catshark *Foxc2* and *Zic1* and found that, as in tetrapods, both are expressed throughout the sclerotome (Fig. 1a, b). During median fin development, their expression domains extend dorsally and ventrally into the median finfolds (Fig. 1a, b; Supplementary Figs 3a, b and 4a, b). We also examined *Scleraxis* (sclerotome-related helix-loop-helix type transcription factor), a marker of the sclerotomal sub-compartment (syndetome) that forms axial tendons in chick and mouse^{17,18}. Catshark *Scleraxis* marks a similar subset of the sclerotome and, like *Foxc2* and *Zic1*, its expression domain extends into the median finfolds (Fig. 1c; Supplementary Figs 3c and 4c). Strong expression of all three sclerotomal markers persisted during differentiation of the fin radials and neural arches.

To determine whether cells from the dermomyotome and neural crest also participate in median fin development, we examined *Pax7*, a marker of these cell types in other vertebrate embryos¹⁹. *Pax7* was initially expressed in the catshark dermomyotome and dorsal neural tube, but *Pax7*-expressing cells were not detected in the median fin before stage 31 (Fig. 1d; Supplementary Figs 3d and 4d). *Pax7* expression then extended from the dermomyotome into the median fins, in the muscle projections lateral to the developing skeleton (Fig. 1d; Supplementary Fig. 3d). Immunolocalization of Zn12, a neural crest marker²⁰, revealed that a limited number of neural crest cells also invaded these fins, but most of the mesenchyme was negative for this marker (Fig. 1e; Supplementary Fig. 3e). By stage 31, Zn12 had localized predominantly to the space within the AEF, where dermal rays develop, and subjacent to the distal ectoderm (Fig. 1e; Supplementary Fig. 3e). Together our results suggest that the bulk of the median fin mesenchyme is derived from sclerotome, although cells from dermomyotome and neural crest also contribute to median fin development (Fig. 1f; Supplementary Fig. 3f). If technical challenges can be overcome, cell labelling in shark embryos will further address the contributions of these cell types.

During limb development, lateral plate mesoderm is regionalized into limb-forming and non-limb-forming domains by differential expression of *Hox* and *Tbx* genes^{3,4}. We investigated whether anteroposterior regionalization of the median finfold into dorsal, anal and caudal regions involves similar mechanisms. In catsharks, median fins lie posterior to the cloaca, suggesting that, if *Hox* genes are involved in their development, then the most likely candidates would be *AbdB*-related *Hox9–Hox13* genes. Therefore, we cloned 5' *Hoxd* genes from catsharks and examined their expression during median fin development (Fig. 2 and Supplementary Figs 5 and 6). Prior to the extension of sclerotome towards the dorsal and ventral finfolds, we observed collinear expression of *Hoxd9*, *Hoxd10*, *Hoxd12* and *Hoxd13* in the somitic mesoderm (Supplementary Fig. 6). The *Hoxd9* domain extended anterior to the cloaca, marking the region in which median fin outgrowth was

¹Department of Zoology, ²Department of Anatomy and Cell Biology, University of Florida, PO Box 118525, Gainesville, Florida 32611, USA.

maintained (Supplementary Figs 1 and 6). For *Hoxd9* and *Hoxd10*, we observed different anterior boundaries in the neural tube, paraxial, intermediate and lateral plate mesoderm (Supplementary Fig. 6). The mesenchymal component of the finfold had developed by stage 25, and *Hoxd* genes were expressed in an anteroposteriorly-nested pattern along the dorsal and ventral finfolds, with specific combinations characterizing first dorsal, second dorsal and anal fin levels (Fig. 2a, b). The first dorsal fin region was characterized by expression of *Hoxd9* and *Hoxd10*, whereas the second dorsal and anal regions were distinguished by additional expression of *Hoxd12* (Fig. 2a, b). *Hoxd13* remained confined to the caudal fin region (Fig. 2a, b).

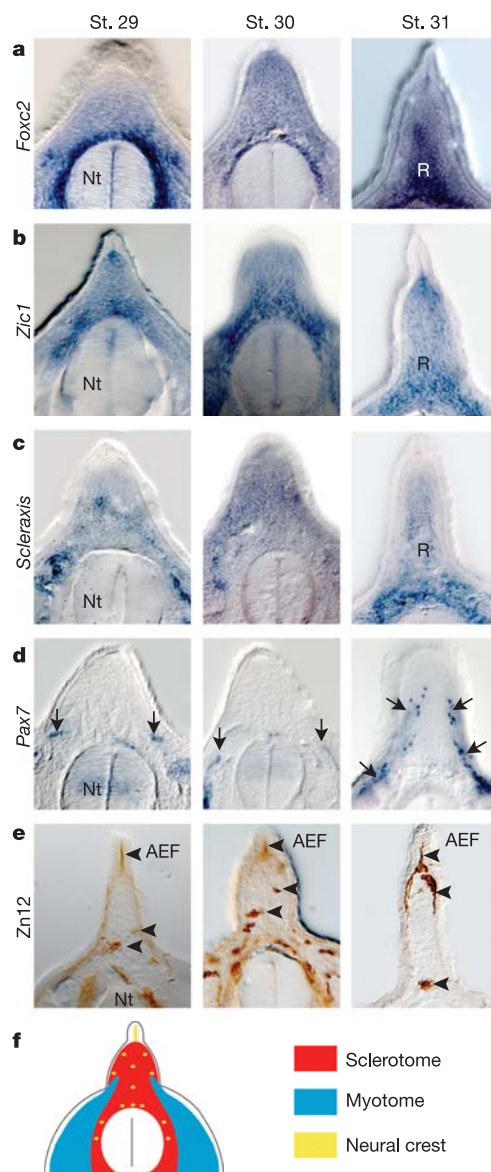


Figure 1 | Developmental origin of catshark median fins. Transverse sections through first dorsal fins; dorsal is to top. Developmental stage (St.) indicated at top. **a–c**, Expression of *Foxc2* (**a**), *Zic1* (**b**) and *Scleraxis* (**c**) in sclerotome surrounding the neural tube (Nt), and in dorsal midline mesenchyme invading the median fins. At stage 31, the strongest expression of *Foxc2* and *Scleraxis* is detected in the developing fin radials (R). **d**, *Pax7* expression in the dorsal lip of the dermomyotome (arrows, stages 29 and 30), and later in myotomal projections invading the median fins (arrows, stage 31). **e**, Isolated *Zn12*-positive neural crest cells (arrowheads) in median fin mesenchyme and within the apical ectodermal fold (AEF). **f**, Schematic summary of the cellular contributions to the dorsal median fins.

As individual fins emerged from the finfold, *Hoxd* gene expression persisted in the developing fins but was downregulated in the adjacent somites (Fig. 2c). In the first dorsal fin, *Hoxd9* and *Hoxd10* expression was maintained, and *Hoxd12* and *Hoxd13* were activated sequentially (Figs 2c and 3a). The second dorsal and anal fins expressed *Hoxd10*, *Hoxd12* and subsequently *Hoxd13*, but *Hoxd9* expression had shifted anteriorly out of these fins by stage 30 (Fig. 2c). These patterns are consistent with the hypothesis that combinatorial expression of *Hoxd* genes may establish a molecular map for median fin position and identity²¹.

It is unlikely that *Hox* genes act alone to specify fin and limb position. Recent work has implicated *Tbx18* in defining anterior boundaries of forelimbs and somites in chick embryos⁴. To examine whether this gene may also relate to boundary formation in median

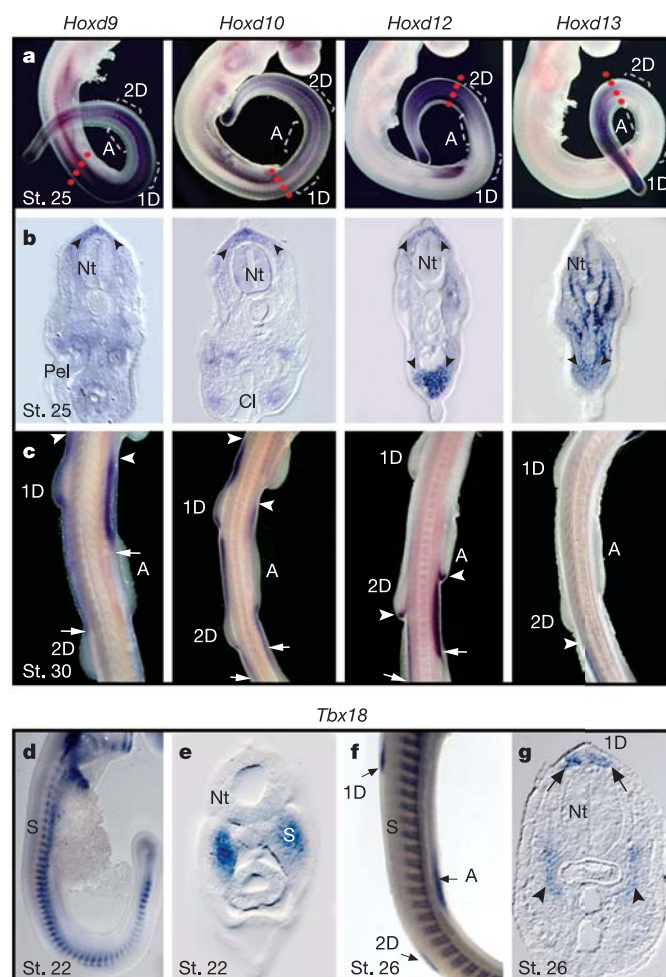


Figure 2 | Regionalized expression of *Hoxd* genes and *Tbx18* along the median finfold of catsharks. Developmental stage indicated in lower left corners. Dorsal is to top in sections and left in whole-mounts. **a**, *Hoxd* gene expression in stage 25 embryos. Brackets indicate regions of prospective first dorsal (1D), second dorsal (2D) and anal (A) fins. Red dotted lines indicate anterior expression boundaries in the median finfold, as verified by histological sections. **b**, Transverse sections immediately posterior to dotted lines in **a** showing *Hoxd* gene expression in dorsal and ventral midline mesenchyme beneath the AEF (arrowheads). Pel, pelvic fin; Cl, cloaca; Nt, neural tube. **c**, *Hoxd* gene expression during emergence of individual median fins at stage 30. Arrowheads mark anterior and arrows mark posterior boundaries of *Hoxd* expression in dorsal and ventral finfolds. **d**, **e**, Expression of *Tbx18* in somites (S) in whole-mount (**d**) and transverse section (**e**). **f**, *Tbx18* expression becomes detectable in presumptive dorsal and anal fins at stage 26 (arrows). **g**, Transverse section showing *Tbx18* expression in first dorsal fin (arrows) and in sclerotome (arrowheads).

fin, we cloned and examined expression of a catshark *Tbx18* orthologue. *Tbx18* was first expressed in the anterior region of each somite (Fig. 2d, e). During finfold outgrowth, we detected *Tbx18* in three discrete domains that delineated the prospective first dorsal, second dorsal and the anal fins (Fig. 2f, g), resembling the pattern observed in chick limbs⁴. Given the function of *Tbx18* in specifying limb position in lateral plate mesoderm, we suggest that *Tbx18* may also participate in specification of median fin position within the finfold, further extending the parallel between median and paired fin development.

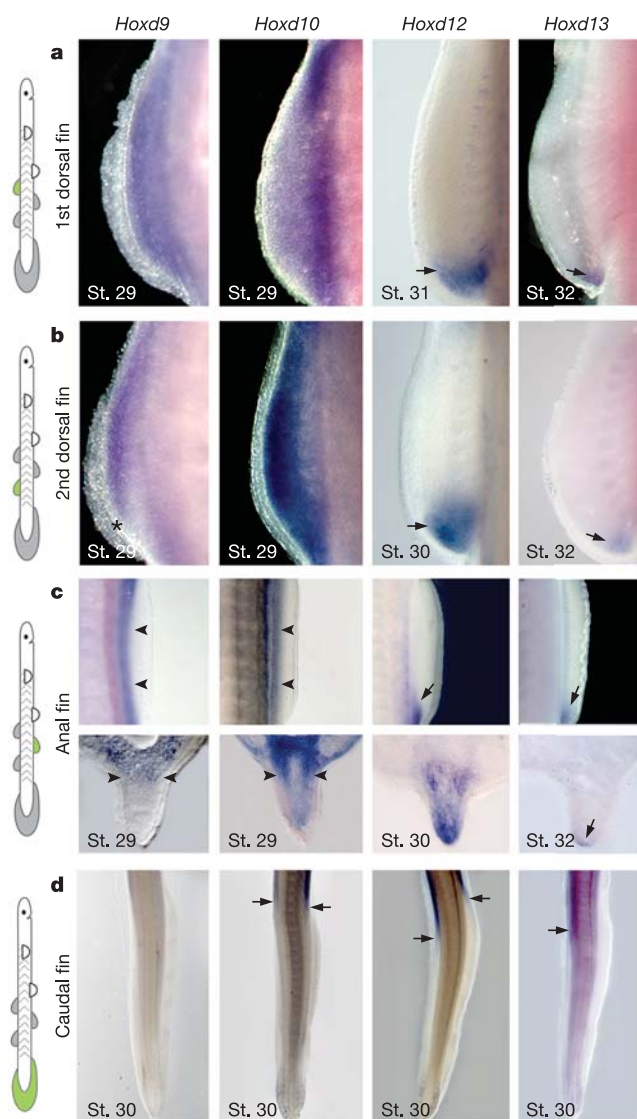


Figure 3 | Anteroposterior nesting of *Hoxd* gene expression in catshark median fin buds. Anterior is to top and dorsal is to left in whole-mounts; dorsal is to top in sections. Stages of development indicated in lower left corners. Diagram to left shows location of fins (green) depicted in adjacent panels. **a**, *Hoxd* expression in first dorsal fins. Arrows point to *Hoxd12* and *Hoxd13* expression at the posterior margin of fin. **b**, *Hoxd* expression in second dorsal fins. Asterisk marks the posterior boundary of *Hoxd9* expression that has started to shift anteriorly. Arrows point to expression of *Hoxd12* and *Hoxd13* at the posterior margin of the fin. **c**, Upper panels show *Hoxd* expression in anal fins, and lower panels show transverse sections through these fins. Arrowheads indicate *Hoxd9* and *Hoxd10* expression along the proximal region of fin. Arrows mark posterior expression of *Hoxd12* and *Hoxd13*. Note temporal and spatial collinearity of *Hoxd* gene expression within the dorsal (**a**, **b**) and anal (**c**) fins. **d**, Caudal fins lacking *Hoxd* expression at stage 30; arrows indicate posterior limits of *Hoxd* expression in the pre-caudal finfolds.

Dorsal and anal fin skeletons are polarized along their antero-posterior axes (Supplementary Fig. 1d, e). In paired limb buds, *Hoxd* genes are expressed along the anteroposterior axis in a spatial and temporally collinear pattern that determines the polarity of the skeleton^{8,9}. We therefore explored whether *Hoxd* expression in each median fin follows the patterns observed in paired limbs. In the first dorsal fin, *Hoxd9* and *Hoxd10* were expressed broadly from the onset of budding (Fig. 3a). *Hoxd12* became detectable posteriorly by stage 31, and *Hoxd13* expression was observed nested within the *Hoxd12* domain one stage later (Fig. 3a). Similar collinear patterns were observed in the second dorsal and anal fins (Fig. 3b, c). Thus, shark dorsal and anal fins exhibit the characteristic collinearity of paired appendages^{22,23}. In contrast to this 'appendicular' pattern of expression in dorsal and anal fins, the caudal fin develops in the absence of *Hoxd* gene expression after stage 30 (Fig. 3d). Posterior expression of 5' *Hoxd*, *Hoxb8* and *Hand2* genes establishes the zone of polarizing activity in paired limbs, which patterns the anteroposterior axis via secretion of Sonic hedgehog⁸. Our finding of a conserved relationship between the polarity of *Hoxd* gene expression and the anteroposterior pattern of the fin skeleton suggests that a similar mechanism may operate in median fins.

Interpretation of these results in the context of fin evolution suggests that the fin development program may have originated in paraxial mesodermally-derived median fins before paired fins evolved in lateral plate mesoderm. To test this hypothesis, we

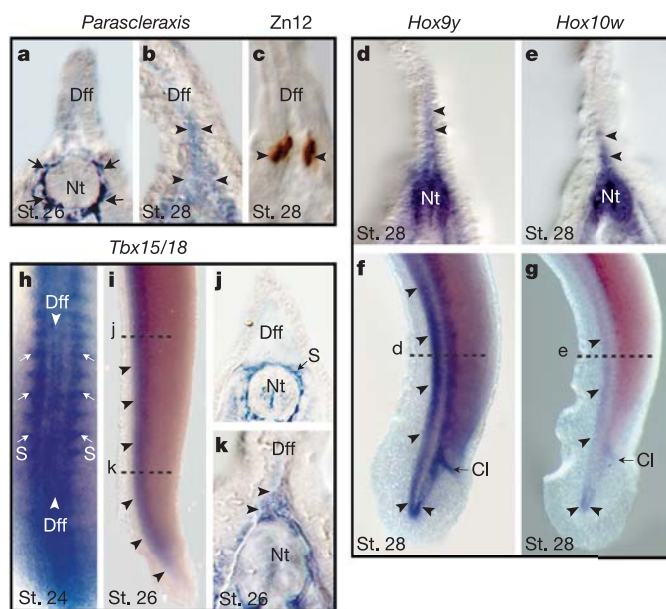


Figure 4 | Lamprey median fin development. Stages of development indicated in lower left corners. **a–e**, **j** and **k** are transverse sections with dorsal to top, **f–i** are whole-mounts with dorsal to left. **a**, Expression of *Parascleraxis* in sclerotome (arrows) adjacent to neural tube (Nt). Dff, dorsal finfold. **b**, *Parascleraxis* expression has expanded into the dorsal finfold (arrowheads). **c**, Zn12 staining in two clusters of cells at the base of the dorsal finfold (arrowheads). **d**, **e**, Expression of *Hox9y* (**d**) and *Hox10w* (**e**) in the dorsal finfold mesenchyme (arrowheads). Note that the fin tissue distal to the expression domains is ectodermal. **f**, **g**, Expression of *Hox9y* (**f**) and *Hox10w* (**g**) in the finfold (arrowheads). Dashed lines mark the approximate planes of sections shown in **d** and **e**. Cl, cloaca. **h**, Expression of *Tbx15/18* in the anterior part of each somite (S; arrows) and in the dorsal finfold (arrowheads) at stage 24. **i**, Expression of *Tbx15/18* in the median finfold at stage 26 (arrowheads). Dashed lines mark approximate planes of sections shown in **j** and **k**. **j**, **k**, Transverse sections taken anterior (**j**) and posterior (**k**) to the expression boundary of *Tbx15/18* in the median finfold. Note that somitic expression extends anterior to the finfold domain (**k**).

extended our analysis to lampreys, which exhibit the plesiomorphic condition of median fins in the absence of paired appendages^{2,10}. During lamprey embryogenesis, a single ectodermal median finfold develops along the entire trunk. Proximodistal expansion of finfold mesenchyme occurs predominantly in the posterior region, where median fins differentiate during metamorphosis²⁴. To determine whether median fins of lampreys and sharks have the same embryonic origin, we isolated and characterized the expression of a lamprey *Scleraxis* orthologue. Phylogenetic analysis of our full-length clone placed it as the sister to the gnathostome *Scleraxis*/*Paraxis* clade, and therefore we designated it *Parascleraxis* (Supplementary Fig. 7). *Parascleraxis* expression was detected at stage 26 in sclerotomal cells adjacent to the neural tube but not in dermomyotome (Fig. 4a). By stage 28, the *Parascleraxis* domain extended into the median finfold, consistent with a sclerotomal contribution to lamprey median fins (Fig. 4b). Restriction of *Parascleraxis* to the lamprey sclerotome also suggests that the dermomyotomal domain of *Paraxis* in gnathostomes may be a novel site of expression that was acquired after duplication of the ancestral *Parascleraxis* gene gave rise to *Paraxis* and *Scleraxis*. We then stained lamprey embryos for Zn12, as previous workers reported migration of neural crest cells into the lamprey median finfold^{25,26}. Zn12 signal was detected in two clusters of sub-epidermal cells at the base of the finfold, and later in a narrow column of cells at its distal tip, but the bulk of median finfold mesenchyme was negative for Zn12 (Fig. 4c and data not shown). These data suggest that, as in sharks, the sclerotome and a limited number of neural crest cells give rise to the median fin mesenchyme of lampreys.

We next asked whether anteroposterior boundaries of median fins in lampreys and sharks are specified by an evolutionarily conserved mechanism involving 5' *Hox* and *Tbx18* orthologues. We analysed the expression of lamprey *Hox9y* and *Hox10w* (ref. 27), and detected expression of both genes in the median finfold mesenchyme (Fig. 4d, e). The anterior boundary of *Hox9y* expression in the dorsal finfold and adjacent somites extended anterior to the *Hox10w* domain and delineated the region in which dorsal fin outgrowth is sustained during larval development (Fig. 4f, g). We also screened for a lamprey *Tbx18* orthologue and isolated a complementary DNA fragment that our phylogenetic analyses joined to the base of the gnathostome *Tbx15/18* clade (Supplementary Fig. 8). Lamprey *Tbx15/18* was expressed anteriorly in each somite and in the median finfold at stage 24 (Fig. 4h). Expression in the median finfold mesenchyme remained posterior, in the fin-forming region, whereas the somitic expression extended along the entire trunk at stage 26 (Fig. 4i–k).

Conservation of the embryonic origin and the patterns of *Hox* and *Tbx* gene expression in shark and lamprey median fins suggests that the molecular mechanisms of fin development evolved in the midline before the origin of paired fins. Our finding that median fin mesenchyme arises predominantly from somites suggests that these cells may acquire their positional identities, in the form of *Hox* and *Tbx* expression, during regionalization of paraxial mesoderm. We suggest that the origin of paired appendages from lateral plate mesoderm involved re-deployment of mechanisms that were originally restricted to paraxial mesoderm, where they regulated development of cartilage (*Hox9–Hox13*, *Tbx18*), muscle (*Pax7*, *Paraxis*) and tendon (*Scleraxis*) in the axial skeleton and median fins. Reports of *Msx* and *Dlx* expression in paired and median fins of zebrafish^{28,29} may reflect additional evolutionary signatures of this co-option. It is possible that the mechanisms of fin and limb development were established in median finfolds even before the origin of vertebrates. Analysis of median finfold development in cephalochordates will further test the hypothesis that these mechanisms emerged early in chordate evolution.

METHODS

Isolation of catshark and lamprey genes. Degenerate polymerase chain reaction with reverse transcription (RT–PCR) was performed to amplify catshark

fragments of 5' *Hoxd* genes (*Hoxd9*, 387 base pairs, bp; *Hoxd10*, 813 bp; *Hoxd12*, 561 bp; *Hoxd13*, 579 bp), *Tbx18* (534 bp), *Zic1* (204 bp), *Foxc2* (267 bp) and *Pax7* (294 bp) using cDNA from a stage 28 *Scyliorhinus canicula*. A full-length copy of catshark *Scleraxis* (1,413 bp) was obtained by RT–PCR and 5' rapid amplification of cloned ends (RACE). Lamprey genes (*Tbx15/18* and *Parascleraxis*) were isolated by RT–PCR from a *Petromyzon marinus* cDNA library (a gift from J. Langeland) using Advantage GC-PCR Kit (Clontech). The amplified fragments were cloned into pGEM-T Easy Vector (Promega) or pDrive Cloning Vector (Qiagen). Orthology of the cloned sequences was determined by protein alignment comparisons followed by maximum-likelihood and neighbour-joining methods.

Whole-mount *in situ* hybridization and immunocytochemistry. These were performed as described previously³⁰. Antibodies against Fgf8 (Santa Cruz Biotechnology Inc), Distal-less (Dll/Dlx; kindly supplied by G. Boekhoff-Falk) and Zn12 (Developmental Studies Hybridoma Bank) were diluted to working concentrations of 1:100, 1:70 and 1:5 respectively. Peroxidase-conjugated secondary antibodies (DAKO) were diluted to 1:500 in phosphate buffered saline (PBS) with 1% Triton and 1% serum. Following whole-mount *in situ* hybridization or immunocytochemistry, the specimens were equilibrated in graded sucrose in PBS (15% and 30%) at 4 °C and graded gelatine in PBS (20% gelatine in 30% sucrose and 20% gelatine) at 50 °C. Embryos were then mounted in Tissue-Tek OCT (Sakura Finetek) and cryosectioned at 20–35 µm.

Received 26 July 2005; accepted 19 June 2006.

Published online 26 July 2006.

1. Zhang, X. G. & Hou, X. G. Evidence for a single median fin-fold and tail in the Lower Cambrian vertebrate, *Haikouichthys ercaicunensis*. *J. Evol. Biol.* **17**, 1162–1166 (2004).
2. Coates, M. I. The origin of vertebrate limbs. *Development (Suppl.)*, 169–182 (1994).
3. Cohn, M. J. *et al.* *Hox9* genes and vertebrate limb specification. *Nature* **387**, 97–101 (1997).
4. Tanaka, M. & Tickle, C. *Tbx18* and boundary formation in chick somite and wing development. *Dev. Biol.* **268**, 470–480 (2004).
5. Saunders, J. W. The proximo-distal sequence of origin of parts of the chick wing and the role of the ectoderm. *J. Exp. Zool.* **108**, 363–403 (1948).
6. Grandel, H. & Schulte-Merker, S. The development of the paired fins in the zebrafish (*Danio rerio*). *Mech. Dev.* **79**, 99–120 (1998).
7. Grandel, H., Draper, B. W. & Schulte-Merker, S. *dackel* acts in the ectoderm of the zebrafish pectoral fin bud to maintain AER signaling. *Development* **127**, 4169–4178 (2000).
8. Zakany, J., Kmita, M. & Duboule, D. A dual role for *Hox* genes in limb anterior-posterior asymmetry. *Science* **304**, 1669–1672 (2004).
9. Turchini, B. & Duboule, D. Control of *Hoxd* genes collinearity during early limb development. *Dev. Cell* **10**, 93–103 (2006).
10. Donoghue, P. C. J., Forey, P. L. & Aldridge, R. J. Conodont affinity and chordate phylogeny. *Biol. Rev. Camb. Philos. Soc.* **75**, 191–251 (2000).
11. Sun, X., Mariani, F. V. & Martin, G. R. Functions of FGF signalling from the apical ectodermal ridge in limb development. *Nature* **418**, 501–508 (2002).
12. Tucker, A. S. & Slack, J. M. Independent induction and formation of the dorsal and ventral fins in *Xenopus laevis*. *Dev. Dyn.* **230**, 461–467 (2004).
13. Smith, M., Hickman, A., Amanze, D., Lumsden, A. & Thorogood, P. Trunk neural crest origin of caudal fin mesenchyme in the zebrafish *Brachydanio rerio*. *Proc. R. Soc. Lond. B* **256**, 137–145 (1994).
14. Sobkow, L., Epperlein, H. H., Herklotz, S., Straube, W. L. & Tanaka, E. M. A germline GFP transgenic axolotl and its use to track cell fate: dual origin of the fin mesenchyme during development and the fate of blood cells during regeneration. *Dev. Biol.* **290**, 386–397 (2006).
15. Furumoto, T. A. *et al.* Notochord-dependent expression of MFH1 and PAX1 cooperates to maintain the proliferation of sclerotome cells during the vertebral column development. *Dev. Biol.* **210**, 15–29 (1999).
16. Sun Rhodes, L. S. & Merzdorf, C. S. The *zic1* gene is expressed in chick somites but not in migratory neural crest. *Gene Expr. Patterns* **6**, 539–545 (2006).
17. Brent, A. E., Schweitzer, R. & Tabin, C. J. A somitic compartment of tendon progenitors. *Cell* **113**, 235–248 (2003).
18. Brent, A. E. & Tabin, C. J. FGF acts directly on the somitic tendon progenitors through the Ets transcription factors *Pea3* and *Erm* to regulate scleraxis expression. *Development* **131**, 3885–3896 (2004).
19. Lacosta, A. M., Muniesa, P., Ruberte, J., Sarasa, M. & Dominguez, L. Novel expression patterns of Pax3/Pax7 in early trunk neural crest and its melanocyte and non-melanocyte lineages in amniote embryos. *Pigment Cell Res.* **18**, 243–251 (2005).
20. Trevarrow, B., Marks, D. L. & Kimmel, C. B. Organization of hindbrain segments in the zebrafish embryo. *Neuron* **4**, 669–679 (1990).
21. Mabee, P. M., Crotwell, P. L., Bird, N. C. & Burke, A. C. Evolution of median fin modules in the axial skeleton of fishes. *J. Exp. Zool.* **294**, 77–90 (2002).
22. Sordino, P., Van der Hoeven, F. & Duboule, D. *Hox* gene expression in teleost fins and the origin of vertebrate digits. *Nature* **375**, 678–681 (1995).

23. Nelson, C. E. *et al.* Analysis of Hox gene expression in the chick limb bud. *Development* **122**, 1449–1466 (1996).
24. Richardson, M. K. & Wright, G. M. Developmental transformations in a normal series of embryos of the sea lamprey *Petromyzon marinus* (Linnaeus). *J. Morphol.* **257**, 348–363 (2003).
25. Hirata, M., Ito, K. & Tsunekuni, K. Migration and colonization patterns of HNK-1-immunoreactive neural crest cells in lamprey and swordtail embryos. *Zool. Sci.* **14**, 305–312 (1997).
26. McCauley, D. W. & Bronner-Fraser, M. Neural crest contributions to the lamprey head. *Development* **130**, 2317–2327 (2003).
27. Force, A., Amores, A. & Postlethwait, J. H. Hox cluster organization in the jawless vertebrate *Petromyzon marinus*. *J. Exp. Zool.* **294**, 30–46 (2002).
28. Akimenko, M. A., Ekker, M., Wegner, J., Lin, W. & Westerfield, M. Combinatorial expression of three zebrafish genes related to *distal-less*: part of a homeobox gene code for the head. *J. Neurosci.* **14**, 3475–3486 (1994).
29. Akimenko, M. A., Johnson, S. L., Westerfield, M. & Ekker, M. Differential induction of four *msx* homeobox genes during fin development and regeneration in zebrafish. *Development* **121**, 347–357 (1995).
30. Freitas, R. & Cohn, M. J. Analysis of *EphA4* in the lesser spotted catshark identifies a primitive gnathostome expression pattern and reveals co-option during evolution of shark-specific morphology. *Dev. Genes Evol.* **214**, 466–472 (2004).

Supplementary Information is linked to the online version of the paper at www.nature.com/nature.

Acknowledgements We thank A. Burke, P. Mabey, P. Crotwell and B. Shockey for commenting on the manuscript, A. Graham for sharing reagents, and L. Page and G. Weddle for assistance with lamprey collection. R. Freitas is a PhD student of the GABBA Program (ICBAS, Univ. Oporto) and was supported by a fellowship from FCT, Praxis XXI.

Author contributions R.F. performed and designed (with M.J.C.) the reported studies. G.Z. performed part of the gene cloning and phylogenetic analyses. M.J.C. supervised the research project, and assisted in the experimental design. R.F. and M.J.C. wrote the manuscript. All authors discussed the results and commented on the manuscript.

Author Information Reprints and permissions information is available at www.nature.com/reprints. Sequences for *Foxc2*, *Zic1*, *Scleraxis*, *Pax7*, *Hoxd9*, *Hoxd10*, *Hoxd12*, *Hoxd13* and *Tbx18* from *S. canicula*, and *Parascleraxis* and *Tbx15/18* from *P. marinus*, are deposited in GenBank under accession numbers DQ659101–DQ659111. The authors declare no competing financial interests. Correspondence and requests for materials should be addressed to M.J.C. (cohn@zoo.ufl.edu).

Supplement to: Evidence that mechanisms of fin development evolved in the midline of early vertebrates

Renata Freitas¹, GuangJun Zhang¹ and Martin J. Cohn^{1,2}

¹Department of Zoology, ²Department of Anatomy and Cell Biology, University of Florida, P.O. Box 118525, Gainesville, FL 32611

Contents: Supplementary Methods, Supplementary Figures and Legends (1-8).

SUPPLEMENTARY METHODS

Collection of embryos

Lesser spotted catshark eggs (*Scyliorhinus canicula*) were collected from Menai Strait (North Wales, UK). Embryos were isolated from egg cases and dissected from the yolk sac in ice-cold phosphate buffered saline (PBS). Fertilized eggs from mountain brook lamprey (*Ichthyomyzon greeleyi*) were collected from the Ohio River (West Virginia, USA) and embryos were cultured in filtered river water. Catshark and lamprey embryos were staged according to Ballard *et al.*¹ and Tahara², respectively.

Scanning electron microscopy and histology

Catshark embryos were prepared for scanning electron microscopy as previously described³. For histology, embryos were dehydrated in graded ethanol series, washed in xylene and embedded in paraffin wax. Sections were cut at 10 µm, dewaxed in xylene and rehydrated before staining with hematoxylin and eosin.

Whole-mount cartilage staining

Embryos were fixed in 95% ethanol, then washed in 70% acid ethanol (70% ethanol with 1% HCl) and transferred to 0.1% alcian green in 70% acid ethanol for 2-4 hours. Stained specimens were differentiated in several washes of acid ethanol before being dehydrated in 100% ethanol and cleared in Benzyl Alcohol:Benzyl Benzoate (1:2).

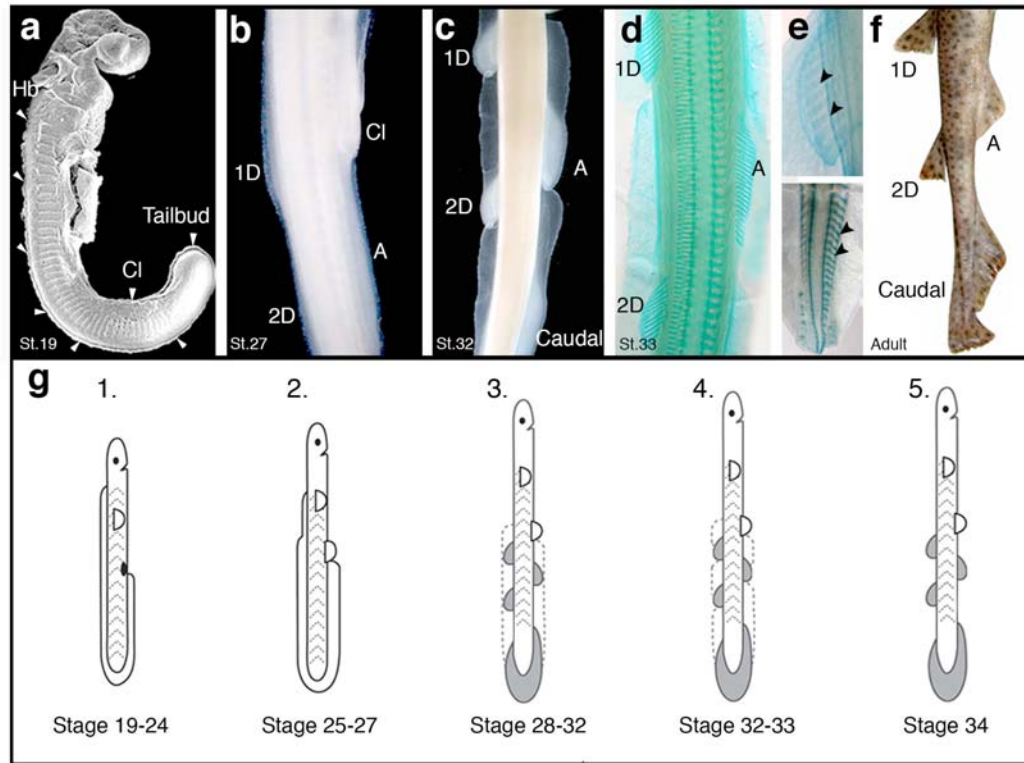
Sequence analyses

Multiple sequence alignments were generated for each gene cloned and their related sequences available in the GenBank using CLUSTAL X⁴ software. Catshark *Hoxd* genes were compared with the vertebrate consensus sequences in order to identify residues diagnostic of paralogy groups⁵. Phylogenetic analyses of each multiple protein alignment were conducted with maximum-likelihood⁶ and neighbor-joining⁷ methods using TREE-PUZZLE and MEGA3 software, respectively.

REFERENCES

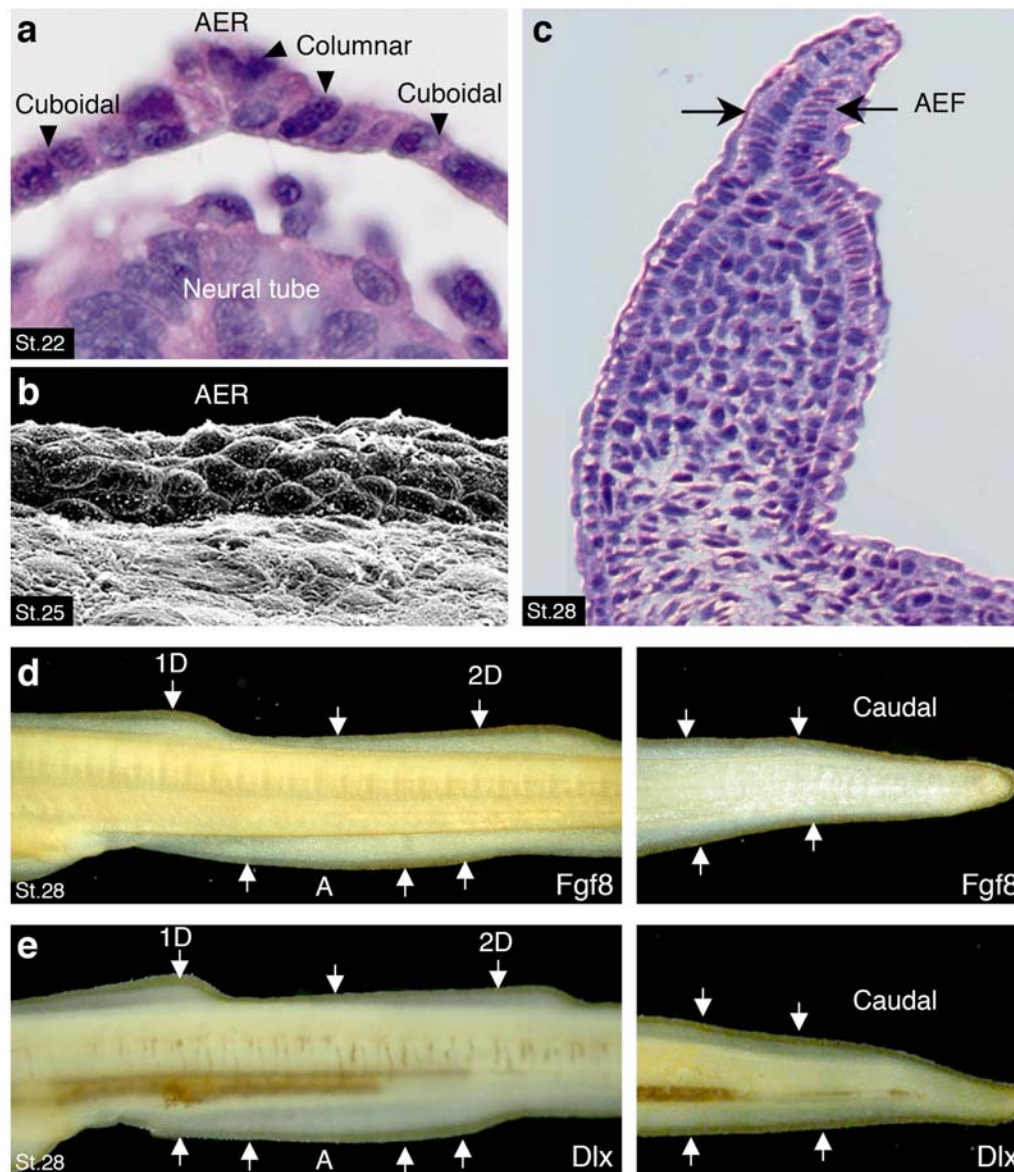
1. Ballard, W. W., Mellinger, J. & Lechenault, H. A series of normal stages for development of *Scyliorhinus canicula*, the Lesser Spotted Dogfish (Chondrichthyes: Scyliorhinidae). *The Journal of Experimental Zoology* **267**, 318-336 (1993).
2. Tahara, Y. Normal stages of development in the lamprey. *Lampetra reissneri* (Dybowski). *Zool Sci* **5**, 109-118 (1988).
3. Freitas, R. & Cohn, M. J. Analysis of *EphA4* in the lesser spotted catshark identifies a primitive gnathostome expression pattern and reveals co-option during evolution of shark-specific morphology. *Dev Genes Evol* **214**, 466-72 (2004).
4. Thompson, J. D., Gibson, T. J., Plewniak, F., Jeanmougin, F. and Higgins, D. G. The ClustalX windows interface: flexible strategies for multiple sequence alignment aided by quality analysis tools. *Nucleic Acids Research* **24**, 4876-4882 (1997).
5. Sharkey, M., Graba, Y. & Scott, M. P. *Hox* genes in evolution: Protein surfaces and paralog groups. *Trends in Genetics* **13**, 145-151 (1997).
6. Schmidt, H. A., Strimmer, K., Vingron, M. & von Haeseler, A. TREE-PUZZLE: maximum likelihood phylogenetic analysis using quartets and parallel computing. *Bioinformatics* **18**, 502-4 (2002).
7. Kumar, S., Tamura, K. & Nei, M. MEGA3: Integrated software for molecular evolutionary genetics analysis and sequence alignment. *Brief Bioinform* **5**, 150-63 (2004).

Supplementary Figure 1



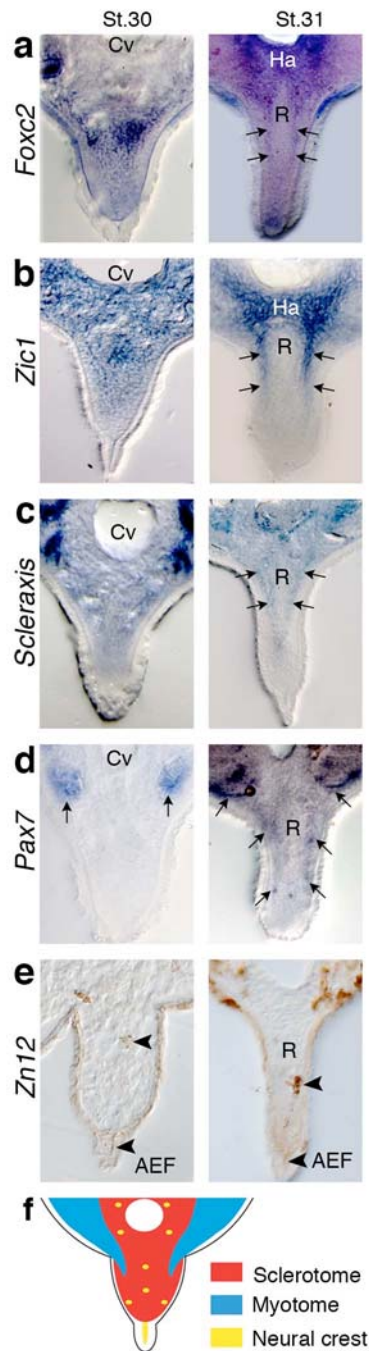
Supplementary Figure 1. Development of catshark median fins. Right lateral views; anterior is towards the top and dorsal is to the left. Stages of development indicated in lower left corners. **a**, Scanning electron micrograph of a catshark embryo showing the initial median finfold along the dorsal and ventral midlines (arrowheads). Hb, hindbrain; Cl, cloacal region. **b**, Light micrograph of median finfold at axial level of the cloaca. 1D, first dorsal fin; 2D, second dorsal fin; A, anal fin. **c**, Development of individual median fin condensations within the finfold. Note that inter-fin regions of the finfold are less dense than the fin-forming regions. **d**, Alcian green stained embryo, showing formation of cartilaginous radials in the median fins but not in the inter-fin regions of the finfold. **e**, Detail of the dorsal (upper panel) and caudal (lower panel) fin skeletons. Note that caudal endoskeletal supports are fused to the axial skeleton while dorsal fin radials are detached from the vertebral column (arrowheads). **f**, Median fins of an adult catshark. **g**, Schematic diagram summarizing five phases of median fin development. **1**, Initiation of a continuous embryonic finfold; **2**, Maintenance of finfold outgrowth posterior to the cloacal level; **3**, Condensation of median fin buds within the finfold; **4**, Division of fin and inter-fin regions; **5**, Degeneration of inter-fin tissue prior to hatching.

Supplementary Figure 2



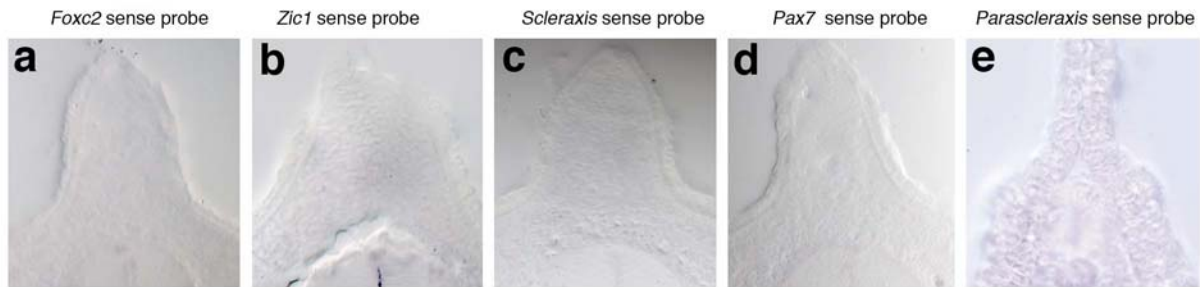
Supplementary Figure 2. Median finfold develops an apical ectodermal ridge (AER). Dorsal is towards the top in all panels and anterior is to the left in **d** and **e**. Stages of development indicated in lower left corners. **a**, Transverse section through the apical ectodermal ridge (AER) of the median finfold. Note differences in shape of epithelial cells in AER and adjacent ectoderm (arrowheads). **b**, Scanning electron micrograph showing AER in the dorsal midline. **c**, Transverse section through the first dorsal fin bud after transition of the AER into an apical ectodermal fold (AEF). **d**, **e**, Immunolocalization of Fgf8 (**d**) and Dlx (**e**) proteins in the AEF of the median finfolds (arrows). 1D, first dorsal fin; 2D, second dorsal fin; A, anal fin.

Supplementary Figure 3



Supplementary Figure 3. Developmental origin of catshark anal fins. Transverse sections through anal fins. Stages of development indicated at top. **a-c**, *Foxc2* (**a**), *Zic1* (**b**) and *Scleraxis* (**c**) are expressed in the sclerotomal cells that invade the anal fin. At stage 31, all three genes are expressed in the differentiating haemal arches (Ha) around the caudal vein (Cv), and in the periphery of the developing radials (R). **d**, *Pax7* is expressed in the dermomyotome at the base of the anal fin at stage 30. At stage 31, *Pax7* is detected in myotomal projections invading the anal fin (arrows). **e**, Immunolocalization of *Zn12* shows isolated clusters of neural crest cells in the anal fin mesenchyme and also within the apical ectodermal fold (AEF) and subjacent to the distal ectoderm (arrowheads).

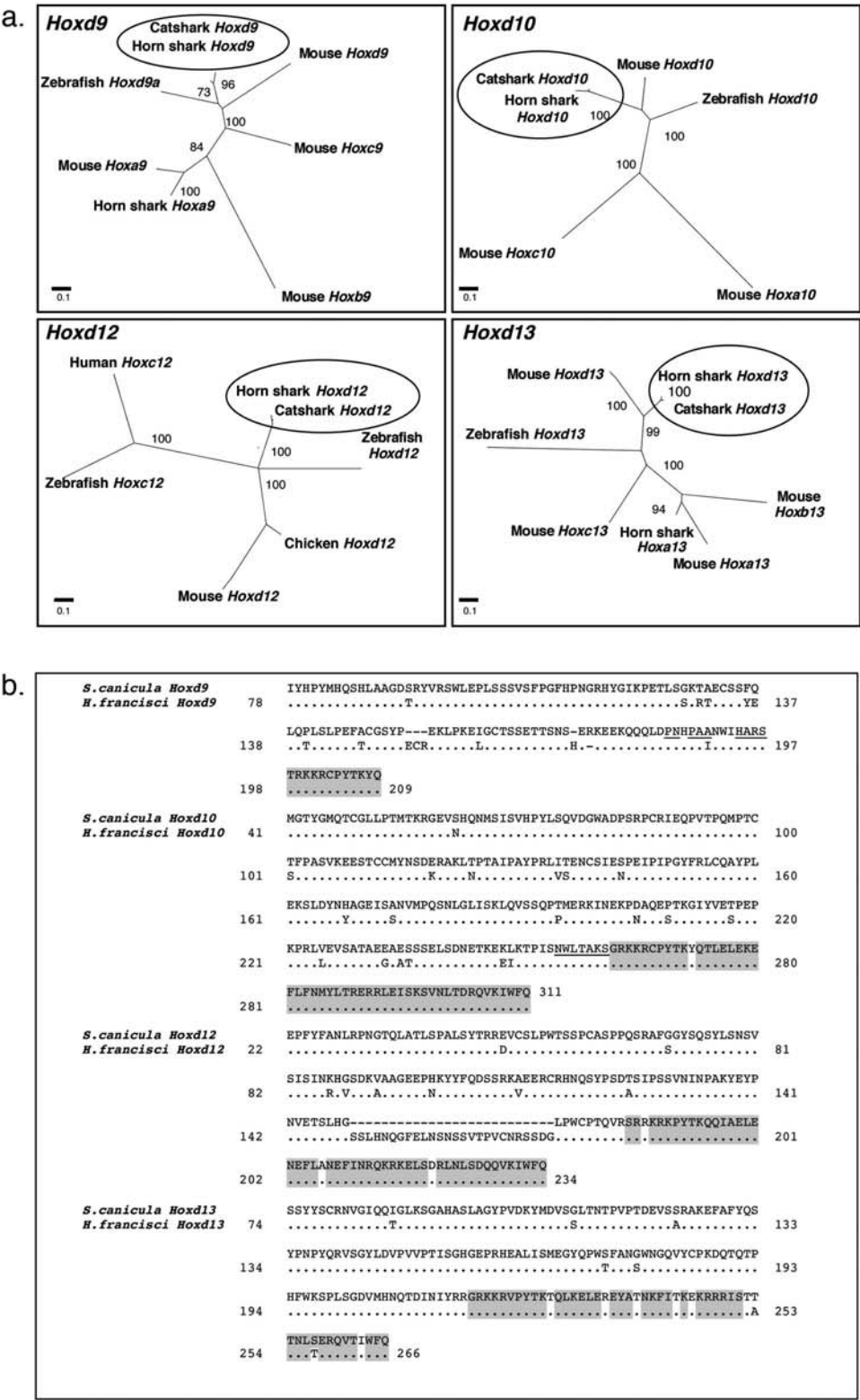
Supplementary Figure 4



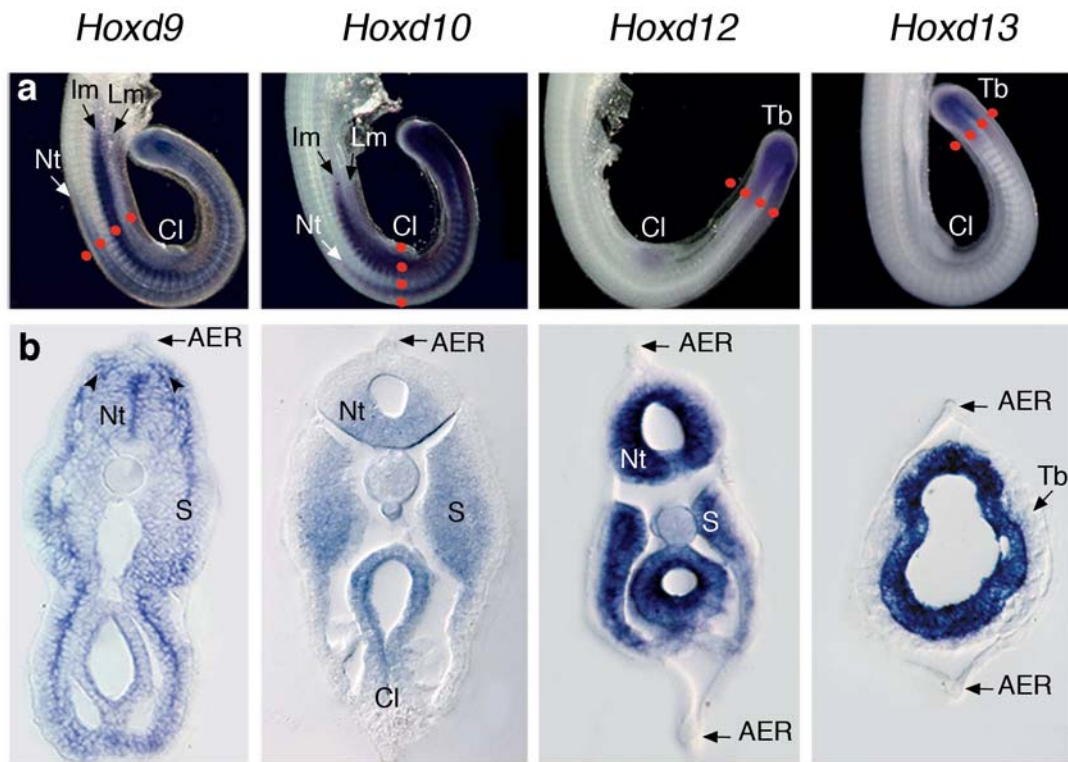
Supplementary Figure 4. Sense controls for *Foxc2*, *Zic1*, *Scleraxis*, *Pax7* and *Parascleraxis*. *In situ* hybridizations of dorsal fins performed with sense RNA probes confirm the specificity of the signal obtained with antisense probes. Compare with Fig. 1 and Supplementary Fig. 3.

Supplementary Figure 5. Phylogenetic analyses of catshark 5'*Hoxd* orthologues. **a**, Maximum-likelihood radial phylograms comparing the deduced amino acid sequences of catshark *Hoxd9*, *Hoxd10*, *Hoxd12* and *Hoxd13* genes with paralogous genes from other vertebrates. The degree of similarity is indicated by branch length, and support values are noted for each branch. Note orthology of catshark and horn shark *Hoxd* genes (circled). **b**, Partial amino acid sequence alignments of AbdominalB (AbdB)-related 5'*Hoxd* genes, in catshark (*S. canicula*) and horn shark (*H. francisci*). Predicted amino acid sequence for each of the *Hoxd* fragments showed highest identity with the *Hoxd* proteins of the horn shark (89% identity for *Hoxd9*, 87% for *Hoxd10*, 77% for *Hoxd12* and 96% for *Hoxd13*). Single dots indicate conserved residues and dashes represent gaps inserted to align homologous residues. Numbers indicate amino acid positions of horn shark sequence. Amino acids that match the vertebrate consensus sequences are shadowed and residues outside the homeodomain, that are diagnostic of paralogy groups, are underlined.

Supplementary Figure 5

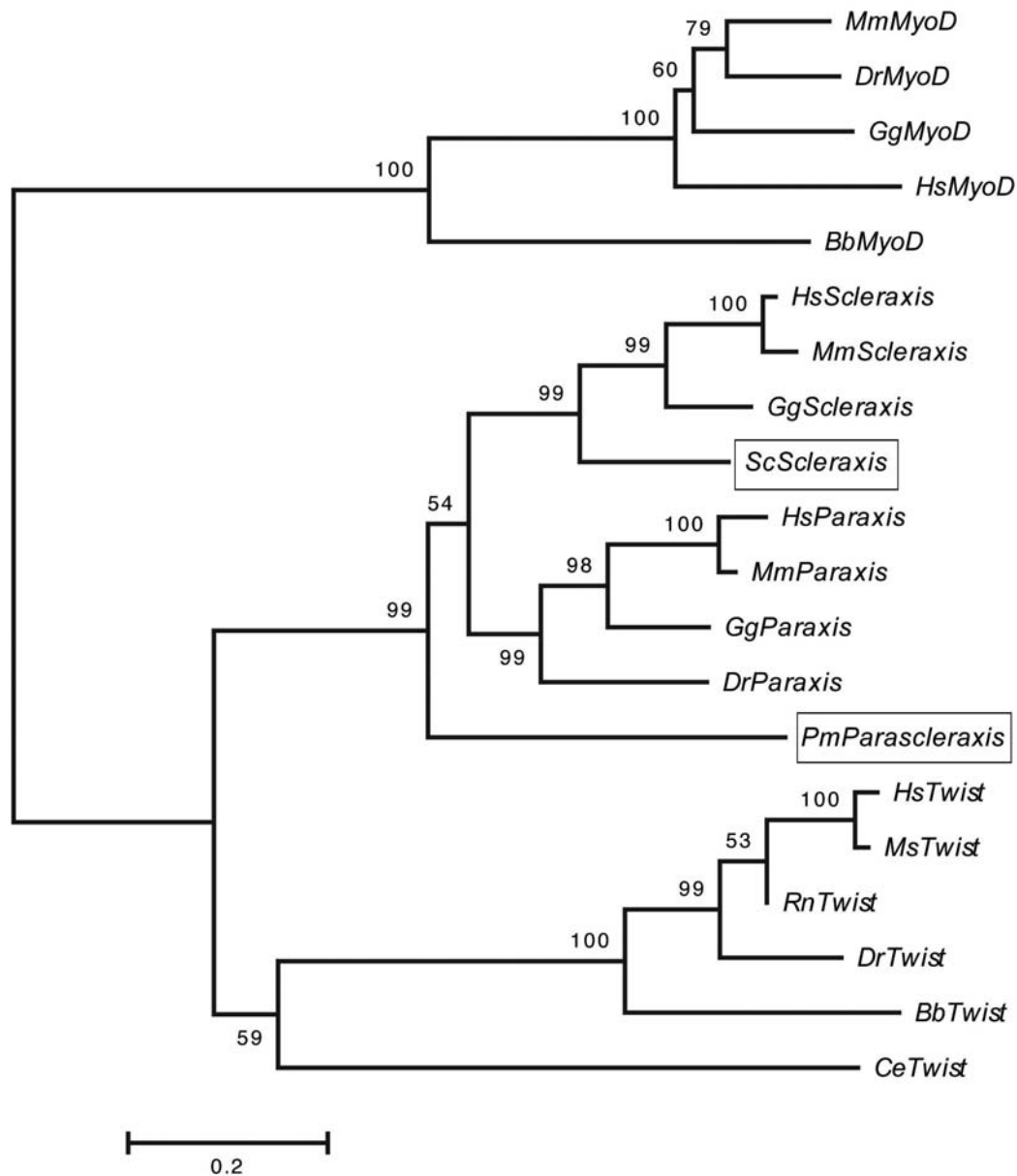


Supplementary Figure 6



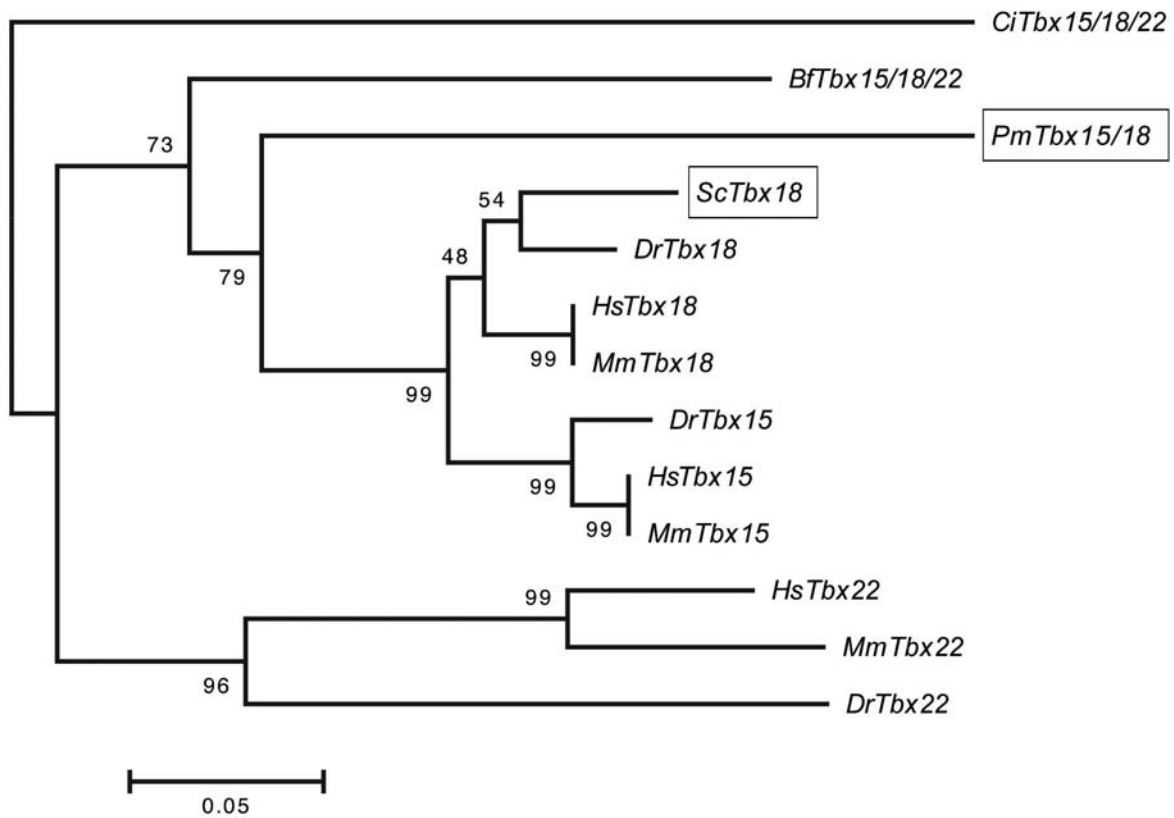
Supplementary Figure 6. Regionalized expression of *Hoxd* genes in catshark embryos at stage 22. **a**, Whole-mount *in situ* hybridizations of *Hoxd9*, *Hoxd10*, *Hoxd12* and *Hoxd13*. Arrows point to staggered anterior boundaries of *Hoxd9* and *Hoxd10* expression in neural tube (Nt), intermediate mesoderm (Im) and lateral plate mesoderm (Lm). Red dotted lines indicate anterior boundaries of *Hoxd* gene expression in the somitic mesoderm. Cl, cloacal region; Tb, tailbud. **b**, Transverse sections taken immediately posterior to dotted lines in **a**. Note that somitic (S) expression of *Hoxd9* at this stage has already extended dorsally around the neural tube (arrowheads) towards the dorsal finfold (Dff). Vff, ventral finfold.

Supplementary Figure 7



Supplementary Figure 7. Phylogenetic analysis of *S. canicula* and *P. marinus* *Scleraxis* orthologues. Neighbor-joining phylogenetic tree of the bHLH transcription factors *Scleraxis*, *Paraxis*, *Twist* and *MyoD* constructed with alignment of deduced amino acid sequences using Mega3 software. Numbers indicate bootstrap scores for each node, based on 10,000 replicates; branch lengths are proportional to the expected replacements per site. *Mm*, *Mus musculus*; *Dr*, *Danio rerio*; *Gg*, *Gallus gallus*; *Hs*, *Homo sapiens*; *Bb*, *Branchiostoma belcheri*; *Sc*, *Scyliorhinus canicula*; *Pm*, *Petromyzon marinus*; *Rn*, *Rattus norvegicus*; *Ce*, *Caenorhabditis elegans*.

Supplementary Figure 8



Supplementary Figure 8. Phylogenetic analysis of *S. canicula* and *P. marinus* Tbx18 orthologues. Neighbor-joining phylogenetic tree of *Tbx15*, *Tbx18* and *Tbx22* constructed with alignment of deduced amino acid sequences and rooted with *Tbx15/18/22* from *Ciona intestinalis*. Numbers indicate bootstrap scores for each node, based on 10,000 replicates, and branch lengths are proportional to the expected replacements per site. *Ci*, *Ciona intestinalis*; *Bf*, *Branchiostoma floridae*; *Pm*, *Petromyzon marinus*; *Sc*, *Scyliorhinus canicula*; *Dr*, *Danio rerio*; *Hs*, *Homo sapiens*; *Mm*, *Mus musculus*.